analytical chemistry

Article

pubs.acs.org/ac

Structural Analysis of an Intact Monoclonal Antibody by Online Electrochemical Reduction of Disulfide Bonds and Fourier Transform Ion Cyclotron Resonance Mass Spectrometry

Simone Nicolardi,* André M. Deelder, Magnus Palmblad, and Yuri E. M. van der Burgt

Center for Proteomics and Metabolomics, Leiden University Medical Center, Albinusdreef 2, 2300 RC Leiden, The Netherlands

Supporting Information

ABSTRACT: Structural confirmation and quality control of recombinant monoclonal antibodies (mAbs) by top-down mass spectrometry is still challenging due to the size of the proteins, disulfide content, and post-translational modifications such as glycosylation. In this study we have applied electrochemistry (EC) to overcome disulfide bridge complexity in top-down analysis of mAbs. To this end, an electrochemical cell was coupled directly to an electrospray ionization (ESI) source and a Fourier transform ion cyclotron resonance (FTICR) mass spectrometer (MS) equipped with a 15 T magnet. By performing online EC-assisted reduction of interchain disulfide bonds in an intact mAb, the released light chains could be selected for tandem mass spectrometry (MS/MS) analysis without interference from heavy-chain fragments. Moreover, the acquisition of full MS scans under denaturing conditions allowed profiling of all abundant mAb glycoforms. Ultrahigh-resolution FTICR-MS measurements provided fully resolved isotopic distributions of intact mAb and enabled the identification of the most abundant adducts and other interfering species. Furthermore, it was found that reduction of interchain disulfide bonds occurs in the ESI source dependent on capillary voltage and solvent composition. This phenomenon was systematically evaluated and compared with the results obtained from reduction in the electrochemical cell.

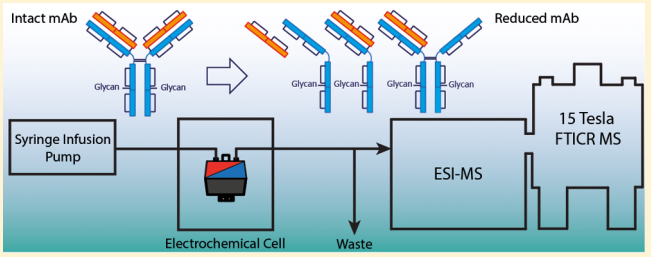

Recombinant monoclonal antibodies (mAbs) form the largest group of modern biotherapeutics. Therapeutic mAbs are used for the treatment of various diseases including cancer, rheumatoid arthritis, autoinflammatory disease, allergic asthma, and multiple sclerosis.[1,2] Recombinant mAbs are large (i.e., ∼150 kDa) proteins that are produced on a large scale using specific immunized and engineered cells lines [e.g., Chinese hamster ovary (CHO) cells].[3,4] Structurally, each mAb can be considered as a protein complex that is composed of two heavy chains and two light chains covalently linked by disulfide bonds between cysteines (i.e., interchain bonds) and arranged in a typical Y-shape to form two fragment antigen binding (Fab) portions and one fragment crystallizable (Fc) portion.[3] The size, nature, and complexity of mAbs pose a challenge for structural confirmation and quality control in the production process. Regulatory authorities, however, require that a biopharmaceutical needs detailed structure analysis during both the production and purification process and that the manufacturer must fulfill to prove the similarity of a biosimilar [see the U.S. Food and Drug Administration (FDA) Web site]. For example, N-glycosylation of the two Fc portions, which has an effect on both the conformation and the biological activity of the mAb, accounts for the largest part of microheterogeneity.[5−8] Mass spectrometry (MS) is these days the method of choice for such analyses. It has played an important role since the early days of manufacturing biopharmaceuticals, and the methods are routinely used to monitor the quality of mAb drug substance and product.[9] The applied MS methods are robust, sensitive, and provide structural information on the analyzed molecule(s) allowing the characterization of among others the amino acid sequence and various post-translational modifications (PTMs).[10−12] With regard to the latter aspect, N-glycosylation is the most extensively studied PTM of mAbs.[13,14] To this end, intact mAbs are analyzed by liquid chromatography (LC) and low-resolution electrospray ionization (ESI)-MS allowing the detection of the most abundant glycoforms and the comparison of different product batches.[15−17] The ESI-MS profiling of intact mAb glycoforms is usually performed under denaturing conditions (i.e., high content of organic solvent and 0.1−1% organic acid) to avoid noncovalent interaction and formation of adduct ions that would complicate the spectra. Alternatively, intact mAbs can be analyzed under native conditions (i.e., no organic solvents and pH 6−7) to determine the protein aggregation level.[18,19] For a more sensitive and detailed analysis of the mAb glycosylation, glycans can be chemically or enzymatically released and profiled after purification by different MS techniques.[20] The mAb can also be enzymatically digested followed by glycopeptide enrichment and detection by MS.[21] The advantage of this latter method is the ability to localize the

Received: January 27, 2014
Accepted: April 29, 2014

 © XXXX American Chemical Society dx.doi.org/10.1021/ac500383c | *Anal. Chem.* XXXX, XXX, XXX−XXX

glycosylation site by tandem mass spectrometry (MS/MS) experiments.[22]

One remaining challenge with regard to structural confirmation of recombinant mAbs is the analysis of disulfide bonds. In a bottom-up procedure for amino acid sequence confirmation, the disulfide bonds are reduced, free cysteines are alkylated, and the protein is digested with an enzyme such as trypsin. Thus, obtained proteolytic peptides are then separated and identified by LC−MS/MS. Note that in such a workflow not only the light chains are separated from the heavy chains, thereby increasing the efficiency of digestion, but that also the intrachain disulfide bonds are reduced. Larger peptides are obtained in a so-called middle-down approach, generally between 20 and 30 kDa, by using enzymes that cleave the mAb at the hinge region.[23,24] To this end, papain cleaves IgG mAbs in the hinge region into two Fab portions and an Fc portion, while the recently developed Ides (or FabRICATOR) cleaves IgG mAbs into an F(ab)2 and an Fc portion and leaves the connectivity between two heavy chains intact. Thus, obtained portions can be sequenced in a middle-down MS/MS experiment. In a middle-up MS procedure the relatively large proteolytic portions of the mAbs can be further separated by LC, digested into smaller peptides, and analyzed by LC−MS.[25] Various research groups in the field of ultrahigh-resolution MS have recently shown the great potential of top-down analysis of intact mAbs. This approach allows the characterization of the amino acid sequence and the localization of PTMs in a single MS experiment.[26,27] Top-down analysis requires mass spectrometers that provide (ultra)high resolving power and accurate mass measurement (HRAM). Such systems have recently become widely available,[28−30] and structure conformation of mAbs is feasible at the intact protein level as recently shown on a time-of-flight (TOF) mass spectrometer, an Orbitrap, and by using Fourier transform ion cyclotron resonance (FTICR).[13,25,31−34] Nevertheless, top-down analysis of intact mAbs can be hampered by the presence of disulfide bonds that reduce the efficiency of fragmentation techniques [i.e., collision-induced dissociation (CID), electron-transfer dissociation (ETD), electron capture dissociation (ECD)] within the protected sequence regions. To overcome this problem, top-down analysis has been performed on the light chains and the heavy chains separated after chemical reduction and alkylation of the cysteines.[13] A recently reported alternative for the reduction of disulfide bonds involves online electrochemistry, as has been exemplified for α- and β-lactoglobulin, lysozyme, oxytocin, and hepcidin.[35−37] Here we report on the electrochemistry (EC)-assisted reduction of disulfide bonds of an immunoglobulin G1 (IgG1) antibody and the power of top-down analysis. For comparison, intact IgG1 was directly infused for ESI-FTICR analysis with or without using an EC cell for reduction. It was found that the interchain connectivities between the light and the heavy chains of the mAb could be disassembled, thus allowing top-down analysis of the light chain.

EXPERIMENTAL SECTION

Chemicals. Stock solutions of an IgG1 monoclonal antibody were kindly provided by Roche Diagnostics GmbH (Germany) and contained 5 mM histidine, 60 mM trehalose, and 0.01% (v/v) Tween 20. From this stock, new solutions of mAb were prepared in Milli-Q water to obtain a concentration of approximately 6.8 μM. This solution was further aliquoted in microcentrifuge tubes (50 or 250 μL) and stored at −80 °C until further use. Working solutions of the IgG1 (~0.13 μM) were prepared in 50%, 10%, and 4.75% (v/v) acetonitrile (ACN, Sigma HPLC grade) with 0.025%, 0.05%, 0.1%, or 1.0% (v/v) formic acid (FA, Sigma) for immediate analysis.

EC/ESI-FTICR-MS. Direct infusion (DI) ESI-FTICR experiments were performed on a Bruker 15 T solariX FTICR mass spectrometer (Bruker Daltonics, Bremen, Germany) using two different setups. In the first setup, samples were directly infused into the ESI source at 50 μL/h using a syringe infusion pump. In the second setup (see Figure 1), an electrochemical cell with

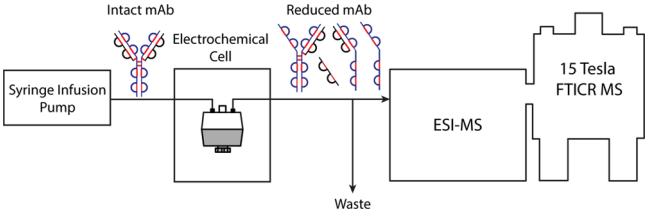

Figure 1. Schematic experimental setup for the MS analysis of intact and reduced mAb using an ultrahigh-resolution FTICR mass spectrometer. In this setup, the reduction of disulfide bonds was obtained using an electrochemical cell online with the FTICR-MS system.

titanium-based electrodes (μ-PrepCell, cell volume 11 μL; Antec, Zoeterwoude, The Netherlands) controlled by a potentiostat (Roxy potentiostat, Antec) was connected between the syringe pump and the ESI source in an online way, i.e., EC/ESI-FTICR-MS. To this end, optimal solvent ratios and acid concentrations were determined with optimized settings (i.e., times) according to manufacturer guidelines, namely, a pulse setting with a 1990 ms interval for "E1", followed by a 1010 ms interval for "E2". Activation of the cell was carried out regularly. To perform reduction of disulfide bond(s) in intact mAb, samples were infused through the EC cell at 50 μL/min and into the ESI source at ~50 μL/h using a microsplitter (Upchurch Scientific). The ESI dry gas flow rate, drying temperature, and nebulizer gas pressure were 3.0 L/min, 200 °C, and 0.8 bar, respectively. The capillary voltage was set to either to −4000, −3000, or −2500 V (as discussed further in this manuscript). The ion funnel 1 operated at 150 V with rf amplitude of 130 Vpp; the skimmer 1 operated at 125 V. The optimal transmission of ions with high m/z values was obtained operating the different multipoles (i.e., the octapole, the quadrupole, and the hexapole) at low radio frequencies and high rf amplitudes. Ions were transmitted through the octapole without any trapping. The analyzer entrance was maintained at −15 V, and side kick technology was used to further optimize peak shape and signal intensity. The optimum excitation power setting was 35% with a pulse time of 10 μs. Typically, low-resolution ESI-FTICR-MS spectra were acquired in the m/z range from 483 to 5000 using the broad-band detection mode with either 64K or 128K data points while ultrahigh-resolution spectra were acquired from m/z 2392.94 to m/z 5000 and from m/z 2024.80 to m/z 5000 with 2 and 1 M data points, respectively. Continuous accumulation of selected ions (CASI) was used to limit the FTICR measurement to a specific m/z range, reducing the number of ions into the ICR cell and improving the quality of the spectra. Finally, MS/MS experiments were performed by CID and fragment ion mass analysis in the ICR cell in the m/z range from 483 to 5000 using the broad-band detection mode with 1 M data points. To

dx.doi.org/10.1021/ac500383c | Anal. Chem. XXXX, XXX, XXX−XXX

this end, ions were accumulated in the hexapole collision cell for 10 s with an isolation window of 25 Da and fragmented using collision voltage of −38 V. All spectra were visualized and processed using DataAnalysis 4.2 (Bruker Daltonics). Deconvolution of low-resolution spectra was performed using the Maximum Entropy tool in DataAnalysis 4.2 while resolved isotopic distributions were deconvolved using the Peptide/Small Mol. tool.

RESULTS AND DISCUSSION

Analysis of Intact IgG1 by ESI-FTICR-MS. The most obvious method to analyze intact IgG1 is direct infusion ESI-MS, preferably using (ultra)high-resolution instrumentation such as TOF, Orbitrap, or FTICR. However, under typical ESI conditions, interpretation of MS data of an intact antibody can be difficult due to the presence of adducts and/or other interfering species, as has been discussed earlier.[38] For unambiguous analysis of intact IgG1, funnel 1 and skimmer 1 voltages, infusion and dry gas flow rates, and nebulizer gas pressure required optimization (see the Experimental Section). Furthermore, ESI-MS of intact mAb yielded different charge state distributions that changed with the amount of organic solvent and acid in solution. As depicted in Figure 2A, ESI-MS analysis of IgG1 under semidenaturing conditions (i.e., 5% ACN and 0.025% FA) resulted in two different charge state distributions, namely, the first in the m/z range of 2500−3750 and the second in the m/z range of 4000−5000. These distributions correspond to different fold states of mAb molecules.[39,40] Complete denaturation of the protein complex was achieved by diluting the mAb in 50% ACN and 0.05% FA. As depicted in Figure 2B, under these conditions, ESI-MS analysis of the IgG1 antibody resulted in the formation of a single charge state distribution, corresponding to unfolded intact mAb. The deconvolved spectrum of this charge state distribution is depicted in Figure S1A in the Supporting Information.

The IgG1 mAb antibody consists of two (identical) light chains of 214 amino acids and two (identical) heavy chains of 449 amino acids.[41] Each light chain (Lc) is covalently linked to one heavy chain (Hc) by one disulfide bond. Two and four intrachain disulfide bonds are present within the light and heavy chains, respectively (see inset Figure 2B). The elemental composition of the resulting protein complex is $C_{6448}H_{9948}N_{1720}O_{2012}S_{44}$ (molecular weight 145165 kDa, monoisotopic mass 145075.67 Da). The complexity of the molecule is further increased as a result of N-glycosylation at Asn-300 in the two heavy chains.[21] The most abundant glycoforms of the $[M + 55H]^{55+}$ ion form of intact IgG1 detected at low-resolution (128K data points) ESI-FTICR-MS under denaturing conditions are depicted in Figure 2C. Note microheterogeneity of the mAb, since various glycan structures can be attached to the two heavy chains, as is shown in the right inset. For example, the most abundant intact mAb glycoform observed in the spectrum contained one G1F glycan on one Hc and one G0F glycan on the other Hc. The theoretical average mass of 147910, 148056, 148218, 148380, 148543, 148705 Da was calculated using the Sequence Editor tool (Bruker Daltonics) for the G0 + G0F, G0F + G0F, G1F + G0F, G1F + G1F, G2F + G1F, and G2F + G2F intact mAb glycoforms, respectively. This calculation must be considered only as an approximation since the average mass of a large molecule like a mAb can be determined only with limited accuracy.[42] Moreover, diluted IgG1 samples were infused without any

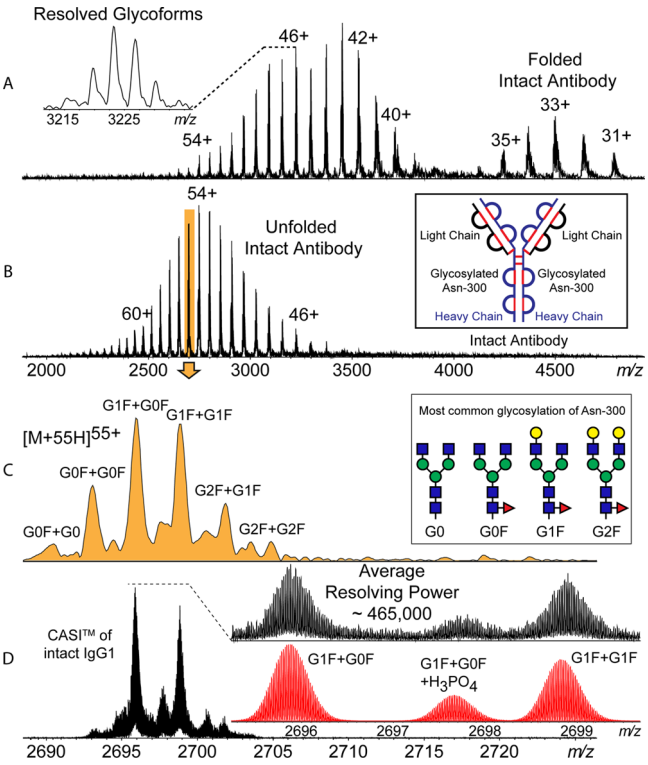

Figure 2. (A) Low-resolution direct infusion ESI-FTICR-MS spectrum of intact mAb under semidenaturing conditions (5% ACN, 0.025% FA). The observed charge state distributions generated from the ionization of the protein complex with different folding states. For each charge state, the most abundant glycoforms of the mAb were resolved. (B) Low-resolution direct infusion ESI-FTICR-MS spectrum of intact mAb under denaturing conditions (50% ACN, 0.05% FA). The observed charge state distribution generated from the unfolded mAb. The schematic of the mAb structure with the light chains, the heavy chains, and the disulfide bonds is depicted in the right inset. (C) Enlargement of the spectrum in panel B with the observed most abundant glycoforms of the 55+ charge state of the intact mAb. These glycoforms generated from the glycosylation of the heavy chains with different combination of the glycan structures depicted in the right inset. (D) Ultrahigh-resolution ESI-FTICR-MS spectrum obtained using continuous accumulation of selected ions (CASI) of intact mAb. The spectrum was obtained from a transient of 10.9 s with seven signal beats and from 421 acquisitions. The enlargement of the spectra shows the unit baseline resolution of the isotopic distributions at ~465 000 average resolving power. Observed and calculated isotopic distributions were compared and used to identify the glycoforms G1F + G0F and G1F + G0F, and the G1F + G0F + H_3PO_4 adduct.

previous (online) purification and/or desalting step; thus, adducts may still be present. The averaged mass of the six detected glycoforms was 147918, 148062, 148222, 148381, 148545, 148711 Da, respectively. A higher deviation from the theoretical mass was observed in the deconvoluted spectrum (Supporting Information Figure S1A). In general, the distribution of detected glycoforms was in good agreement with those previously reported by other authors for an IgG1 mAb.[14,16,43]

Ultrahigh-resolution ESI-FTICR measurements were carried out to identify the most abundant interfering species visible in the low-resolution spectrum. As depicted in Figure 2D, the two most abundant glycoforms of the $[M + 55H]^{55+}$ ion form of the IgG1, namely, G1F + G0F and G1F + G1F, were measured with unit mass baseline resolution of the isotopic distributions

dx.doi.org/10.1021/ac500383c | Anal. Chem. XXXX, XXX, XXX−XXX

at approximately 465 000 resolving power. This allowed the calculation of the mass distances between the different species, namely, a mass difference of 98.99 ± 1.00 Da was observed between the isotopic distributions at m/z range from 2695.4 to 2696.4 and from 2697.3 to 2698.2 (see enlargement in Figure 2D), most likely a H_3PO_4 adduct (theoretical mass 97.98 Da). The identification of such species facilitated exclusion of possible degradation products of the mAb.

Reduction of Intact IgG1 under Positive Ion Mode ESI Conditions. ESI-FTICR-MS spectra of the mAb were acquired with either low (5%) or high percentages (50%) of ACN using a capillary voltage of −3000 and −4000 V, respectively. All other MS parameters were kept constant for the two experiments. Resulting spectra are depicted in Figure 2, parts A and B. Under semidenaturing conditions, lower capillary voltage (i.e., −3000 V) was needed to avoid the fragmentation of the intact mAb during ESI. Interestingly, upon increasing the capillary voltage to −4000 V reduction of disulfide bonds was observed. As is shown in Figure 3A, this S−S reduction under ESI conditions resulted in opening the interchain linkages between the light and the heavy chains leading to the formation of different reduction products, namely, one light chain linked to two heavy chains (Lc + 2Hc), one light chain linked to one heavy chain (Lc + Hc), a heavy chain (Hc) only, and a light chain only (Lc) (for illustrations see the upper-right corner of Figure 3; the deconvolved spectrum of Figure 3A is depicted in Figure S1B in the Supporting Information). The most abundant reduction products in the spectrum were Lc and Lc + Hc, distributed over different charge states resulting in multiple overlapping signals in the spectrum. This overlap hampered the evaluation of the glycoform distributions: only species observed in overlap-free m/z regions were assigned, as is exemplified and depicted in the left panel in Figure 3B for the Lc + Hc. Here, four isoforms of the 30+ charge state of Lc + Hc are shown. These proteoforms were assigned as Lc + Hc complexes modified with G0, G0F, G1F, and G2F glycan, respectively, and with corresponding theoretical average mass of 73882, 74028, 74190, and 74352 Da, respectively. As reported for the intact mAb, also for the Lc + Hc, the mass measurement was affected by the presence of adducts; thus, the averaged mass of the four detected glycoforms was 73891, 74030, 74191, 74357 Da, respectively. The glycoform distribution of the Lc + Hc was in good agreement with those previously reported by other authors for the Hc part only.[16,43]

Similar results were obtained from the ESI-MS analysis of IgG1 mAb diluted in 10% ACN and 0.05% FA (data not shown). Direct infusion ESI-FTICR measurement of IgG1 solutions in 5% ACN and either 0.1% or 1.0% FA with the capillary voltage set to −3000 V generated more complexes, and the signals in the mass spectra were difficult to assign. In order to avoid fragmentation of intact mAb diluted in more acidic solutions the capillary voltage was set to −2500 V (data not shown). Finally, ultrahigh-resolution ESI-FTICR-MS analysis of the Lc + Hc glycoforms was performed. The resulting spectrum is shown in Figure 3B. Unit mass baseline resolution of the isotopic distribution was achieved at approximately 263 000 resolving power. Measurement of Lc + Hc at a lower charge state than for the intact mAb allowed a better separation of interfering ions leading to the identification of H_3PO_4 and potassium adducts. Electrospray ionization inherently involves electrochemistry, and electrochemical reactions of analytes during ESI have been reported

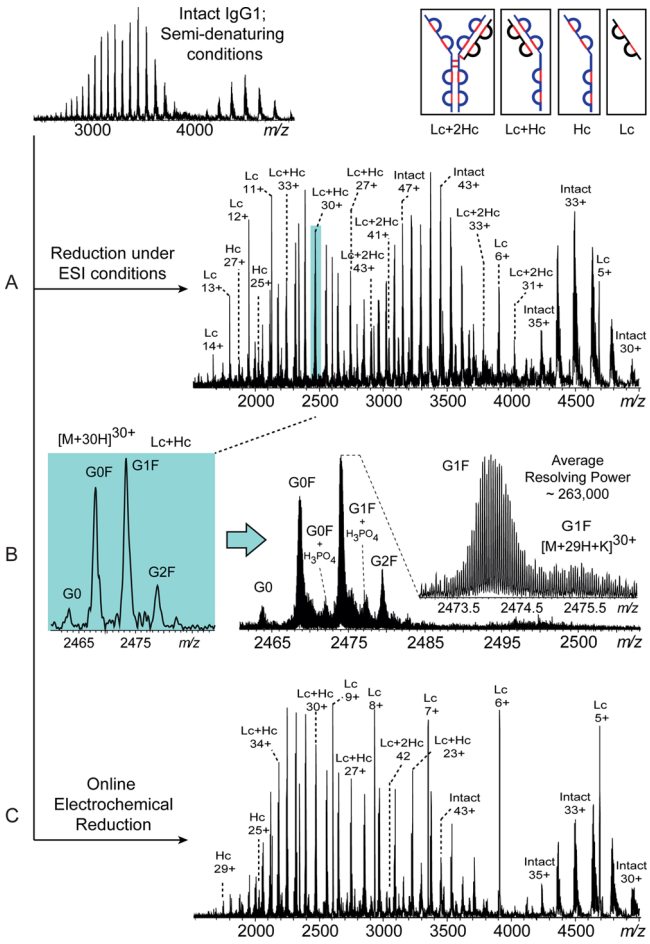

Figure 3. Reduction of interchain disulfide bonds of intact mAb under semidenaturing conditions. (A) Low-resolution ESI-FTICR-MS spectrum of intact and reduced IgG1 obtained using the setup depicted in Figure 1 with capillary voltage of −4000 V. Under these ESI conditions, the mAb fragmented in the Lc + 2Hc, the Lc + Hc, the Hc, and the Lc corresponding to the species depicted in the upper-right corner. (B) Enlargement of the spectrum in panel A with the observed most abundant glycoforms and adducts of the 30+ charge state of the Lc + Hc reduction product (right). Ultrahigh-resolution ESI-FTICR-MS spectrum obtained using CASI of the same glycoforms and adducts (middle left). The enlargement of the spectrum shows the unit baseline resolution of the isotopic distribution of the 30+ charge state of the G1F and the G1F + K glycoforms at ~263 000 average resolving power. (C) Low-resolution ESI-FTICR-MS spectrum of intact and online electrochemically reduced mAb obtained using the setup depicted in Figure 1. The reduction of the interchain disulfide bonds produced the same fragments observed in panel A with different charge state distributions and abundances.

previously.[44,45] Oxidations at the spray needle can occur in positive ion mode, but also reduction processes have been described.[46,47] At this point, it is not clear why the mAb is reduced under semidenaturing conditions at high capillary voltages, and further studies are needed to explain this observation. Note that this mAb was not reduced during ESI-MS analysis under denaturing conditions with the capillary voltage set to −4000 V (Figure 2B), thus indicating that the organic solvent also plays an important role. Furthermore, the influence of the design of the ESI source on the reduction process needs to be studied.

Online Electrochemical Reduction of Intact IgG1 mAb. A common approach to analyze heterogeneity in

dx.doi.org/10.1021/ac500383c | Anal. Chem. XXXX, XXX, XXX−XXX

amino acid sequence or PTMs in mAbs starts with off-line chemical reduction and alkylation of the antibody followed by LC−MS analysis of the Lc and the Hc parts.[13,15,16] As an alternative for chemical reduction, recently online electrochemical reduction of disulfide bonds has been reported for the analysis of peptides and proteins.[35,36] In the current study, we have used an online EC setup (see Figure 1) to reduce and analyze the IgG1 mAb. To this end, working solutions of intact IgG1 containing different percentages of ACN and FA were infused through the electrochemical cell at 50 μL/min and analyzed by ESI-FTICR-MS. During direct infusion experiments the EC cell was switched on to reduce the disulfide bonds in the mAb into SH groups. The online reduction of intact IgG1 under denaturing conditions (i.e., 50% ACN and 0.05% FA) resulted in a spectrum that contained many overlapping or unresolved signals. The results did not change when the solution of mAb was infused at different flow rates or when a higher concentration of FA was used (i.e., 0.05%, 0.1%, and 1%). The same was observed using different ESI capillary voltages (i.e., −4000, −3000, and −2500 V). On the contrary, the online electrochemical reduction of intact IgG1 under semidenaturing conditions (i.e., 5% ACN and 0.025% FA, capillary voltage −3000 V) resulted in spectrum depicted in Figure 3C (corresponding deconvolved spectrum is depicted in Figure S1C in the Supporting Information). The reduction efficiency was evaluated for the E1 and E2 potentials of the EC cell set to −1.5, −2.0, −2.5, −3 V and 1.5, 2.0, 2.5, 3 V, respectively. Although the reduction efficiency did not improve between the different experiments, the highest number of observed species and highest total intensity was obtained setting the E1 and the E2 potentials to −2.5 and +2.5 V, respectively. This was probably due to the fact that under our conditions the maximum reduction efficiency was already reached when the E1 and E2 potentials were set to −1.5 and 1.5 V, respectively. The most abundant species in the spectrum were identified as Lc + 2Hc, Lc + Hc, Lc, and Hc, i.e., the same as described in the previous paragraphs (see Figure 3A). A clear difference in the charge state distribution and relative intensity of these species was observed in the two reduction experiments. This can be a result of changes in the composition of mAb solution after the online electrochemical reduction or differences between reduction mechanisms in the two experiments. The signal intensity of the nonreduced intact mAb (e.g., the $[M + 43H]^{43+}$ indicated as "intact 43+") was significantly lower after online electrochemical reduction than after reduction under ESI conditions. This can be due to a different efficiency of either the reduction processes or ionization (i.e., suppression during ESI). No differences were observed between the glycoform distributions of same species in the two different experiments. Furthermore, online electrochemical reduction of intact IgG1 diluted in 5% ACN and 1.0% FA with capillary voltage at −2500 V resulted in a more complex spectrum in which most signals could not be assigned, however, similar to the spectrum obtained from the electrochemical reduction of the mAb diluted in 50% ACN and 0.05% FA (data not shown).

Top-Down MS/MS of the Light Chain after Reduction of Intact IgG1. Variations in inter- and intrachain S−S connectivities may occur during the manufacturing process of therapeutic mAbs, thus affecting their structure, stability, and bioactivity.[48] Examples of opening of disulfide bonds during the production of IgG1 mAbs, potentially followed by closure of new S−S linkages ("reshuffling"), have been reported.[49] Therefore, characterization of disulfide bonds in mAbs is of utmost importance in order to confirm the quality of these biopharmaceutical products. In this context, MS has played a central role leading to the development of different methods for localization and confirmation of disulfide bonds in mAbs.[50−52] Top-down MS has recently emerged as a powerful tool to localize protein PTMs including disulfide bonds in intact mAbs.[33,53] In the current study, the two interchain disulfide bonds of intact IgG1, namely, between the cysteine at the C-terminus (Cys214) of the light chain and Cys223 of the heavy chain, were reduced in two different ways, namely, during the ESI process or by EC-assisted reduction (see Figure 1). Such a reduction allowed the detection of "free" Lc parts (see Figure 3, parts A and C) and its characterization by top-down ESI-FTICR-MS/MS. It should be noted that the Lc part of the mAb furthermore contains two intrachain disulfide bonds, namely, one in the variable region (Cys28−Cys88) and one in the κ constant region (Cys134−Cys194). The 14+ charge state of the Lc part was selected for top-down CID analysis (Figure 4A).

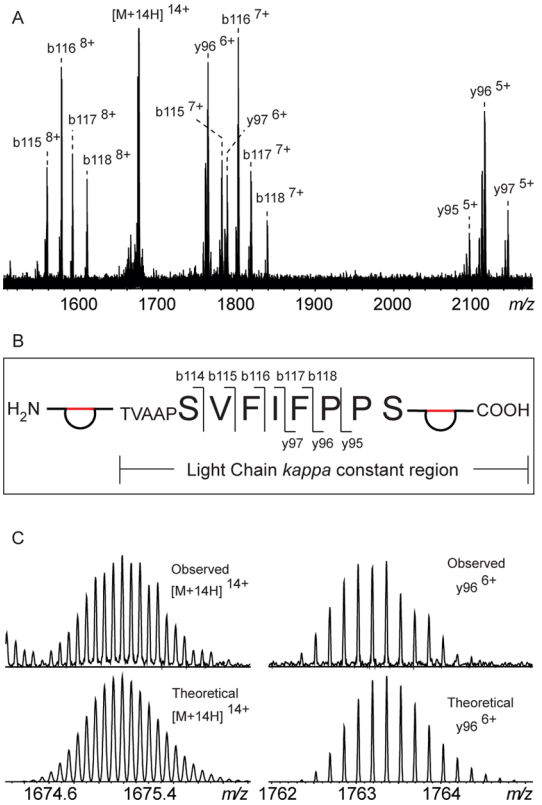

Figure 4. (A) Collision-induced dissociation ESI-FTICR-MS/MS spectrum of the 14+ charge state of the light chain detected after reduction of the interchain disulfide bonds of IgG1 mAb. (B) The detected CID fragment ions resulted from the breakage of peptide bonds in a region corresponding to the beginning of the κ constant region. (C) The observed and calculated isotopic distribution of the $[M + 14H]^{14+}$ precursor ion and the y_{96}^{6+} fragment ion considering four oxidized cysteines were compared to confirm the presence of two disulfide bonds.

Note that in this context "top-down" indicates that no enzymes were used prior to sequencing, whereas this MS/MS experiment could also have been named "middle-down" since only a portion of the mAb is sequenced. In agreement with previous reports, it was found that the presence of (remaining) intrachain disulfide bonds hampered the analysis to obtain full sequence coverage. However, the identified *b*- and *y*-type

dx.doi.org/10.1021/ac500383c | Anal. Chem. XXXX, XXX, XXX−XXX

fragment ions are still sufficient to localize one of the two disulfide bonds. As depicted in Figure 4B, the light chain mainly fragmented in a region corresponding to the beginning of the κ constant region and between the two theoretical intrachain connections. Thus, the presence of a disulfide bond between the two cysteines in the variable regions was confirmed while the assignment or exclusion of a possible connection between either the Cys134 or Cys194 with the C-terminal cysteine was not possible. In fact, small *y*-type fragment ions that would have confirmed the presence of the reduced cysteine at the C-terminus were not detected. The presence of two disulfide bonds in the light chain was confirmed by comparing the observed and calculated isotopic distribution of the precursor ion and the y_{96} fragment ion. As depicted in Figure 4C, the observed isotopic distributions were in good agreement with those calculated considering four oxidized cysteines. As a final remark, it should be emphasized that only few charge states of the Lc parts could be isolated for top-down ESI-FTICR-MS/MS experiments due to multiple overlapping signals in the spectra and that the fragmentation of the 14+ charge state resulted into the most informative CID spectrum. Moreover, top-down CID analysis of the Lc + 2Hc, the Lc + Hc, and the Hc parts was limited by several factors such as overlapping species, low signal intensities of precursor ions, limited remaining signal upon using narrow isolation windows, and poor backbone fragmentation efficiency of glycosylated species. As an alternative, ETD experiments were performed; however, these were unsuccessful due to the fact that different operating settings were needed for efficient accumulation and transmission of both positive ions with high m/z values and small fluoranthene anions (data not shown).

CONCLUSIONS

Heavy and light chains of intact IgG1 mAb were disassembled into free Hc and Lc parts, as well as into combinations of these (Lc + Hc; Lc + 2Hc) using EC-assisted reduction of interchain S−S connectivities. Ultrahigh-resolution MS acquisitions were performed online using an ESI-FTICR system equipped with a 15 T magnet. The most abundant glycoforms of intact IgG1 as well as on an Lc + Hc part were profiled. Moreover, the isotopic distributions of intact mAb were fully resolved in FTICR measurements, thus allowing identification of adducts and other interfering species that were present because no upfront mAb purification was performed. The released Lc part was selected for top-down CID characterization, and the presence of two intrachain disulfide bonds that remained intact upon EC-assisted reduction could be confirmed, i.e., one in the variable region (between Cys28 and Cys88) and one in the κ constant region. Finally, somewhat surprisingly, a second type of reduction of interchain disulfide bonds was observed, namely, during ESI at a capillary voltage of −4000 V and semidenaturing spray solvent conditions. Although the background of this reduction is not understood, it allowed the analysis of the glycosylation of an Lc + Hc complex at both low and ultrahigh resolution as well as top-down CID characterization of the released Lc part.

ASSOCIATED CONTENT

Supporting Information

Deconvolved spectra of the charge state distributions shown in Figure 2B and Figure 3, parts A and C, are depicted in Figure S1. This material is available free of charge via the Internet at http://pubs.acs.org.

AUTHOR INFORMATION

Corresponding Author

*Phone: +31-71-5269384. E-mail: s.nicolardi@lumc.nl.

Notes

The authors declare no competing financial interest.

ACKNOWLEDGMENTS

The authors thank Dietmar Reusch from Roche Diagnostics GmbH (Germany) for providing the IgG1 mAb.

REFERENCES

(1) Scott, A. M.; Wolchok, J. D.; Old, L. J. *Nat. Rev. Cancer* **2012**, *12* (4), 278−287.
(2) Shukla, A. A.; Thömmes, J. *Trends Biotechnol.* **2010**, *28* (5), 253−261.
(3) Arnold, J. N.; Wormald, M. R.; Sim, R. B.; Rudd, P. M.; Dwek, R. A. *Annu. Rev. Immunol.* **2007**, *25* (1), 21−50.
(4) Li, F.; Vijayasankaran, N.; Shen, A. Y.; Kiss, R.; Amanullah, A. *mAbs* **2010**, *2* (5), 466−479.
(5) Krapp, S.; Mimura, Y.; Jefferis, R.; Huber, R.; Sondermann, P. *J. Mol. Biol.* **2003**, *325* (5), 979−989.
(6) Tao, M. H.; Morrison, S. L. *J. Immunol.* **1989**, *143* (8), 2595−2601.
(7) Rosati, S.; van den Bremer, E. T.; Schuurman, J.; Parren, P. W.; Kamerling, J. P.; Heck, A. J. *mAbs* **2013**, *5* (6), 917−924.
(8) Zauner, G.; Selman, M. H.; Bondt, A.; Rombouts, Y.; Blank, D.; Deelder, A. M.; Wuhrer, M. *Mol. Cell. Proteomics* **2013**, *12* (4), 856−865.
(9) Berkowitz, S. A.; Engen, J. R.; Mazzeo, J. R.; Jones, G. B. *Nat. Rev. Drug Discovery* **2012**, *11* (7), 527−540.
(10) Mazur, M.; Seipert, R.; Mahon, D.; Zhou, Q.; Liu, T. *AAPS J.* **2012**, *14* (3), 530−541.
(11) Thompson, N. J.; Rosati, S.; Rose, R. J.; Heck, A. J. R. *Chem. Commun.* **2013**, *49* (6), 538−548.
(12) Wang, L.; Amphlett, G.; Lambert, J.; Blättler, W.; Zhang, W. *Pharm. Res.* **2005**, *22* (8), 1338−1349.
(13) Bondarenko, P.; Second, T.; Zabrouskov, V.; Makarov, A.; Zhang, Z. *J. Am. Soc. Mass Spectrom.* **2009**, *20* (8), 1415−1424.
(14) Damen, C. W. N.; Rosing, H.; Schellens, J. H. M.; Beijnen, J. H. *J. Pharm. Biomed. Anal.* **2008**, *46* (3), 449−455.
(15) Dillon, T. M.; Bondarenko, P. V.; Rehder, D. S.; Pipes, G. D.; Kleemann, G. R.; Ricci, M. S. *J. Chromatogr., A* **2006**, *1120*, 112−120.
(16) Damen, C. W. N.; Chen, W.; Chakraborty, A. B.; van Oosterhout, M.; Mazzeo, J. R.; Gebler, J. C.; Schellens, J. H. M.; Rosing, H.; Beijnen, J. H. *J. Am. Soc. Mass Spectrom.* **2009**, *20* (11), 2021−2033.
(17) Kuribayashi, R.; Hashii, N.; Harazono, A.; Kawasaki, N. *J. Pharm. Biomed. Anal.* **2012**, *67*−*68*, 1−9.
(18) Kukrer, B.; Filipe, V.; van, D. E.; Kasper, P. T.; Vreeken, R. J.; Heck, A. J.; Jiskoot, W. *Pharm. Res.* **2010**, *27* (10), 2197−2204.
(19) Rose, R. J.; Damoc, E.; Denisov, E.; Makarov, A.; Heck, A. J. R. *Nat. Methods* **2012**, *9* (11), 1084−1086.
(20) Qian, J.; Liu, T.; Yang, L.; Daus, A.; Crowley, R.; Zhou, Q. *Anal. Chem.* **2007**, *364* (1), 8−18.
(21) Reusch, D.; Haberger, M.; Selman, M. H. J.; Bulau, P.; Deelder, A. M.; Wuhrer, M.; Engler, N. *Anal. Biochem.* **2013**, *432* (2), 82−89.
(22) Olivova, P.; Chen, W.; Chakraborty, A. B.; Gebler, J. C. *Rapid Commun. Mass Spectrom.* **2008**, *22* (1), 29−40.
(23) Wang, B.; Gucinski, A. C.; Keire, D. A.; Buhse, L. F.; Boyne, M. T., II. *Analyst* **2013**, *138* (10), 3058−3065.
(24) Fornelli, L.; Ayoub, D.; Aizikov, K.; Beck, A.; Tsybin, Y. O. *Anal. Chem.* **2014**, *86* (6), 3005−3012.
(25) Ayoub, D.; Jabs, W.; Resemann, A.; Evers, W.; Evans, C.; Main, L.; Baessmann, C.; Wagner-Rousset, E.; Suckau, D.; Beck, A. *mAbs* **2013**, *5* (5), 699−710.
(26) Zhang, J.; Liu, H.; Katta, V. *J. Mass Spectrom.* **2010**, *45* (1), 112−120.

(27) Zhang, Z.; Shah, B. *Anal. Chem.* **2007**, *79* (15), 5723−5729.
(28) Mann, M.; Kelleher, N. L. *Proc. Natl. Acad. Sci. U.S.A.* **2008**, *105* (47), 18132−18138.
(29) Marshall, A. G.; Hendrickson, C. L. *Annu. Rev. Anal. Chem.* **2008**, *1* (1), 579−599.
(30) Zubarev, R. A.; Makarov, A. *Anal. Chem.* **2013**, *85* (11), 5288−5296.
(31) Tsybin, Y. O.; Fornelli, L.; Stoermer, C.; Luebeck, M.; Parra, J.; Nallet, S.; Wurm, F. M.; Hartmer, R. *Anal. Chem.* **2011**, *83* (23), 8919−8927.
(32) Fornelli, L.; Damoc, E.; Thomas, P. M.; Kelleher, N. L.; Aizikov, K.; Denisov, E.; Makarov, A.; Tsybin, Y. O. *Mol. Cell. Proteomics* **2012**, *11* (12), 1758−1767.
(33) Mao, Y.; Valeja, S. G.; Rouse, J. C.; Hendrickson, C. L.; Marshall, A. G. *Anal. Chem.* **2013**, *85* (9), 4239−4246.
(34) Jones, L.; Zhang, H.; Cui, W.; Kumar, S.; Sperry, J.; Carroll, J.; Gross, M. *J. Am. Soc. Mass Spectrom.* **2013**, *24* (6), 835−845.
(35) Kraj, A.; Brouwer, H. J.; Reinhoud, N.; Chervet, J. P. *Anal. Bioanal. Chem.* **2013**, *405* (29), 9311−9320.
(36) Zhang, Y.; Cui, W.; Zhang, H.; Dewald, H. D.; Chen, H. *Anal. Chem.* **2012**, *84* (8), 3838−3842.
(37) Nicolardi, S.; Giera, M.; Kooijman, P.; Kraj, A.; Chervet, J. P.; Deelder, A. M.; Burgt, Y. *J. Am. Soc. Mass Spectrom.* **2013**, *24* (12), 1980−1987.
(38) Valeja, S. G.; Kaiser, N. K.; Xian, F.; Hendrickson, C. L.; Rouse, J. C.; Marshall, A. G. *Anal. Chem.* **2011**, *83* (22), 8391−8395.
(39) Beck, A.; Sanglier-Cianférani, S.; Van Dorsselaer, A. *Anal. Chem.* **2012**, *84* (11), 4637−4646.
(40) Thompson, N. J.; Rosati, S.; Heck, A. J. R. *Methods* **2014**, *65* (1), 11−17.
(41) Harris, R. J.; Kabakoff, B.; Macchi, F. D.; Shen, F. J.; Kwong, M.; Andya, J. D.; Shire, S. J.; Bjork, N.; Totpal, K.; Chen, A. B. *J. Chromatogr. B: Biomed. Sci. Appl.* **2001**, *752* (2), 233−245.
(42) Zubarev, R. A.; Demirev, P. A.; Håkansson, P.; Sundqvist, B. U. R. *Anal. Chem.* **1995**, *67* (20), 3793−3798.
(43) Xie, H.; Chakraborty, A.; Ahn, J.; Yu, Y. Q.; Dakshinamoorthy, D. P.; Gilar, M.; Chen, W.; Skilton, S.; Mazzeo, J. R. *mAbs* **2010**, *2* (4), 379−394.
(44) Abonnenc, M.; Qiao, L.; Liu, B.; Girault, H. H. *Annu. Rev. Anal. Chem.* **2010**, *3*, 231−254.
(45) de la Mora, J. F.; Van Berkel, G. J.; Enke, C. G.; Cole, R. B.; Martinez-Sanchez, M.; Fenn, J. B. *J. Mass Spectrom.* **2000**, *35* (8), 939−952.
(46) Gianelli, L.; Amendola, V.; Fabbrizzi, L.; Pallavicini, P.; Mellerio, G. G. *Rapid Commun. Mass Spectrom.* **2001**, *15* (23), 2347−2353.
(47) Gu, Z.-m.; Ma, J.; Zhao, X.-g.; Wu, J.; Zhang, D. *Rapid Commun. Mass Spectrom.* **2006**, *20* (19), 2969−2972.
(48) Liu, H.; May, K. *mAbs* **2012**, *4* (1), 17−23.
(49) Trexler-Schmidt, M.; Sargis, S.; Chiu, J.; Sze-Khoo, S.; Mun, M.; Kao, Y. H.; Laird, M. W. *Biotechnol. Bioeng.* **2010**, *106* (3), 452−461.
(50) Zhang, W.; Marzilli, L. A.; Rouse, J. C.; Czupryn, M. J. *Anal. Biochem.* **2002**, *311* (1), 1−9.
(51) Li, X.; Wang, F.; Xu, W.; May, K.; Richardson, D.; Liu, H. *Anal. Biochem.* **2013**, *436* (2), 93−100.
(52) Wu, S. L.; Jiang, H.; Lu, Q.; Dai, S.; Hancock, W. S.; Karger, B. L. *Anal. Chem.* **2008**, *81* (1), 112−122.
(53) Cui, W.; Rohrs, H. W.; Gross, M. L. *Analyst* **2011**, *136* (19), 3854−3864.